Photoassisted Decomposition of Dimethyl Methylphosphonate over Amorphous Manganese Oxide Catalysts

Scott R. Segal[†] and Steven L. Suib*[,†,‡,§]

U-60, Department of Chemistry, Department of Chemical Engineering, and Institute of Materials Science, University of Connecticut, Storrs, Connecticut 06269-4060

Xia Tang[||] and Sunita Satyapal[⊥]

United Technologies Research Center, 411 Silver Lane, East Hartford, Connecticut 06108

Received September 22, 1998. Revised Manuscript Received April 22, 1999

The gas-phase decomposition of dimethyl methylphosphonate (DMMP) has been studied over amorphous manganese oxide (AMO) catalysts in the presence of light (∼200−800 nm). The reaction was studied under oxidizing conditions using air at low temperatures (40−70 °C). DMMP and gas-phase products were studied using gas chromatography (GC). DMMP was found to adsorb strongly to the AMO surface and produce small amounts of methanol (MeOH) even in the absence of light. When AMO was irradiated with light of ∼200−800 nm, large amounts of MeOH and CO_2 were initially formed. Following the initial period of high activity, strong deactivation was observed. After the reactions were performed, aqueous extracts from spent AMO were analyzed using ion chromatography (IC). The IC analyses indicated that several products accumulate on the AMO surface. These products include methyl methylphosphonate (MMP) and methylphosphonic acid (MPA). Greater amounts of MMP and MPA are produced after irradiation. Fourier transform infrared (FTIR) spectroscopy was used to examine adsorbed DMMP species on spent AMO. The IR results indicate that DMMP bonds to Mn Lewis acid sites on the AMO surface via the phosphoryl oxygen. On the basis of these results a mechanism is proposed for the adsorption and photoassisted decomposition of DMMP over AMO.

I. Introduction

There is current interest in developing new methods to safely destroy chemical warfare agents (CWAs). Such materials consist of extremely toxic organophosphorus nerve and blistering agents, including Soman (GD), Sarin (GB), and VX. The testing of CWAs in the laboratory is quite hazardous; therefore, studies are typically done using nontoxic simulants such as dimethyl methylphosphonate (DMMP).[1−11] The structure of DMMP is shown in Figure 1. DMMP is a liquid at 298K, having a low vapor pressure (1.05 Torr).[1] The P−O and P−C bonds in DMMP are less reactive than P−F bonds in actual nerve agents. Therefore, the use of DMMP can provide a good measure for monitoring the effectiveness of methods to degrade CWAs.[2]

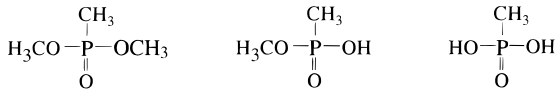

Figure 1. Structures of dimethyl methylphosphonate (DMMP), methyl methylphosphonate (MMP), and methylphosphonic acid (MPA).

An important area recently investigated for CWA decomposition is catalytic oxidation using metals and metal oxides.[1,3−11] Early studies have examined the adsorption and reaction of DMMP vapor with surfaces of metals, including Mo(111) ,[3] Pt(111),[4] Pd(111),[5] and Ni(111),[5] and with metal oxides such as Al_2O_3,[7] SiO_2,[8] Fe_2O_3,[8,9,11] MgO,[11] and La_2O_3.[11] More recently, the catalytic oxidation of DMMP has been studied using Pt/Al_2O_3,[1] Pt/TiO_2/cordierite,[12] and Cu-substituted hydroxyapatite[6] using temperatures between 150 and 500

* To whom correspondence should be addressed.
† Department of Chemistry, University of Connecticut.
‡ Department of Chemical Engineering, University of Connecticut.
§ Institute of Materials Science, University of Connecticut.
|| United Technologies Research Center.

(1) Tzou, T. Z.; Weller, S. W. *J. Catal.* **1994**, *146*, 370−374.
(2) O'Shea, K. E.; Beightol, S.; Garcia, I.; Aguilar, M.; Kalen, D. V.; Cooper, W. J. *J. Photochem. Photobiol. A: Chem.* **1997**, *107*, 221−226.
(3) Smentkowski, V. S.; Hagans, P.; Yates, J. T., Jr. *J. Phys. Chem.* **1988**, *92*, 6351−6357.
(4) Henderson, M. A.; White, J. M. *J. Am. Chem. Soc.* **1988**, *110*, 6939−6947.
(5) Guo, X.; Yoshinobu, J.; Yates, J. T., Jr. *J. Phys. Chem.* **1990**, *94*, 6839−6842.
(6) Lee, K. W.; Houalla, M.; Hercules, D. M.; Hall, W. K. *J. Catal.* **1994**, *145*, 223−231.
(7) Templeton, M. K.; Weinberg, W. H. *J. Am. Chem. Soc.* **1985**, *107*, 97−108.
(8) Henderson, M. A.; Jin, T.; White, J. M. *J. Phys. Chem.* **1986**, *90*, 4607−4611.
(9) Hedge, R. M.; White, J. M. *Appl. Surf. Sci.* **1987**, *28*, 1−10.
(10) Ekerdt, J. G.; Klabunde, K. J.; Shapley, J. R.; White, J. M.; J. T., Jr. *J. Phys. Chem.* **1988**, *92*, 6182−6188.
(11) Mitchell, M. B.; Sheinker, V. N.; Mintz, E. A. *J. Phys. Chem. B.* **1997**, *101*, 11192−11203.

10.1021/cm980664w CCC: $18.00
Published on Web 06/11/1999

°C. In these recent studies,[1,6,12] high DMMP conversions were observed at the beginning of the reactions, with CO_2 and H_2O as major products. Catalyst deactivation due to adsorbed phosphate species then occurs, and methanol was often observed. No P-containing products were observed in the gas phase. HPLC analyses of the spent catalysts or condensates at the ends of the reactor showed the presence of partial DMMP decomposition products, such as dimethyl phosphate, monomethyl phosphate, methyl methylphosphonate, methylphosphonic acid, and phosphoric acid.[1]

Another method currently being investigated for CWA decomposition is photocatalytic oxidation.[2,13] Oxidative photocatalysis has been shown to be effective for decomposing a wide range of toxic organic pollutants,[14] typically using TiO_2. The advantages of this technique are that benign products such as CO_2 and H_2O can be produced, and high temperatures can be avoided. Another advantage of using photocatalysis is that it may be possible to utilize solar energy for reactions.

Many researchers have investigated the photocatalytic decomposition of organophosphorus compounds,[15−17] with several studies examining the photocatalytic decomposition of DMMP.[2,13] In these studies, DMMP was photocatalytically decomposed in aqueous suspensions of TiO_2. Major products included phosphoric acid and CO_2, with intermediates such as methylphosphonic acid, formic acid, and formaldehyde being observed. The researchers proposed that DMMP is degraded through hydroxyl radical-mediated pathways.[2] Recently, the gas-phase photocatalytic decomposition of DMMP was studied over TiO_2 films.[22] In this study, the major products were CO and CO_2 in the gas phase, and MPA and PO_4^{3-} on the catalyst. Deactivation was observed due to the buildup of the P-containing species on the catalyst.[22]

Our research group has been interested in heterogeneous photocatalytic oxidation reactions using manganese oxide catalysts.[18−20] Several gas−solid reactions have been studied including the oxidation of 2-propanol to acetone,[18] and the total oxidation of methyl halides to CO_2.[19] The best catalysts were found to be mixed-valent amorphous manganese oxides (AMO), prepared by the reduction of $KMnO_4$ with oxalic acid.[18−20] The high photocatalytic activity of AMO is due to the ease with which lattice oxygen is readily desorbed.[20] In this work, we have examined gaseous reactions of DMMP over AMO in air. Emphasis has been placed on determining reaction products, examining the role of light, and studying catalyst deactivation. Finally, a mechanism is proposed to explain the interaction of DMMP with AMO.

II. Experimental Section

A. Preparation of Materials. AMO was prepared by a redox reaction involving the reduction of $KMnO_4$ with oxalic acid. A solution containing 1.58 g of $KMnO_4$ (Aldrich, Milwaukee, Wis.) in 100 mL of distilled deionized water (DDW) was mixed with a solution containing 2.26 g of oxalic acid (Fisher, Fair Lawn, NJ) in 100 mL of DDW. The solution was allowed to mix for several hours, which then yielded a dark brownish-black precipitate. The solid was filtered and washed with DDW several times and then dried in an oven at 110 °C overnight. Prior to catalytic reactions, the AMO was ground using a mortar and pestle. DMMP was purchased from Aldrich and was used without further purification.

B. Catalytic Studies. A schematic diagram for the heterogeneous photocatalytic reactor system is shown in Figure 2. A 1000-W Xe arc lamp (Kratos, Schoeffel Instruments, model LPS 255HR Power Supply and LH 151 N lamp housing, Westwood, NJ) was used as the light source. No filters were used; therefore, radiation from the lamp spanned over the entire ultraviolet and visible range (∼200−800 nm). A water bottle was placed between the light source and the reactor to remove heat and infrared radiation. Air was used as the oxidant and was passed through a bubbler containing liquid DMMP, which was kept in a water bath at 25 °C. The flow rate of air was 30 mL/min. Under these conditions, the inlet DMMP concentration is ∼0.14 mol %. The gas was then passed through a stainless steel reactor containing a thin layer (50 mg) of catalyst on a Gelman Sciences glass fiber filter. The reactor temperature was kept at 40 °C, and the outlet lines were heated to 110 °C to prevent condensation of DMMP and other products.

Temperature measurements made inside the reactor indicate that the lamp causes the temperature to increase to 70 °C at the surface of AMO. These measurements were made by loading AMO into the photoreactor. A small hole was made in the glass fiber filter. A narrow thermocouple wire was then directed up from the bottom of the photoreactor through the hole in the filter such that the tip was visible from the top of the reactor and surrounded by AMO.

C. GC Analyses. Reactants and products were analyzed using a Hewlett-Packard 5890 series I gas chromatograph equipped with an automatic gas-sampling valve. A Carbowax 20M capillary column with flame ionization detection was used to analyze for DMMP and methanol. CO_2 was analyzed using a GSC Gas Pro capillary column with thermal conductivity detection. Calibration curves for methanol and CO_2 were prepared from gas standards prepared in our laboratories.

D. FTIR Analyses. Fourier transform infrared (FTIR) spectroscopy (Nicolet Magna-IR 750) was used to examine surface species on the catalysts after reaction. A DTGS detector with a KBr beam splitter was used for analysis over the entire mid-IR range (4000−400 cm^{-1}). The AMO samples were pressed into KBr pellets (2.5% AMO by weight), and transmission spectra were collected.

E. Extraction Analyses of Spent AMO. Soxhlet extractions of spent AMO were performed in $CHCl_3$ and used for analysis of adsorbed DMMP on AMO. The extracts were examined using GC analyses. Aqueous extractions of AMO after DMMP reactions were used to identify methylphosphonic acid (MPA), methyl methylphosphonate (MMP) and phosphates (PO_4^{3-}). The structures of MPA and MMP are shown in Figure 1. The aqueous extracts were prepared by placing the spent AMO in H_2O and treating it with ultrasound for 10 min. The solution was filtered through 0.22 μm filters and analyzed using a Dionex DX 500 ion chromatograph (IC) equipped with a CD 20 conductivity detector and a Dionex AS4A-SC anion exchange column. The eluent used was 1.8 mM Na_2CO_3/1.7 mM $NaHCO_3$ buffer (approximate pH = 10).

(12) Hsu, C. C.; Dulcey, C. S.; Horwitz, J. S.; Lin, M. C. *J. Mol. Catal.* **1990**, *60*, 389−395.
(13) O'Shea, K. E.; Garcia, I.; Aguilar, M. *Res. Chem. Intermed.* **1997**, *23*, 4, 325−339.
(14) Linsebigler, A. L.; Guangquan, L.; J. T., Jr. *Chem. Rev.* **1995**, *95*, 735−758.
(15) Krosley, K. W.; Collard, D. M.; Adamson, J.; Fox, M. A. *J. Photochem. Photobiol. A: Chem.* **1993**, *69*, 357−360.
(16) Grätzel, C. K.; Jirousek, M.; Grätzel, M. *J. Mol. Catal.* **1990**, *60*, 375−387.
(17) Harada, K.; Hisanaga, T.; Tanaka, K. *Water Res.* **1990**, *24*, 11, 1415−1417.
(18) Cao, H.; Suib, S. L. *J. Am. Chem. Soc.* **1994**, *116*, 5334−5342.
(19) Lin, J. C.; Chen, J.; Suib, S. L.; Cutlip, M. B.; Freihaut, J. D. *J. Catal.* **1996**, *161*, 659−666.
(20) Chen, J.; Lin, J. C.; Purohit, V.; Cutlip, M. B.; Suib, S. L. *Catal. Today* **1997**, *33*, 205−214.
(21) Christol, H.; Levy, M.; Marty, C. *J. Org. Chem.* **1968**, *12*, 459−470.
(22) Obee, T. N.; Satyapal, S. *J. Photochem. Photobiol., A: Chem.* **1998**, *118*, 1, 45−51.

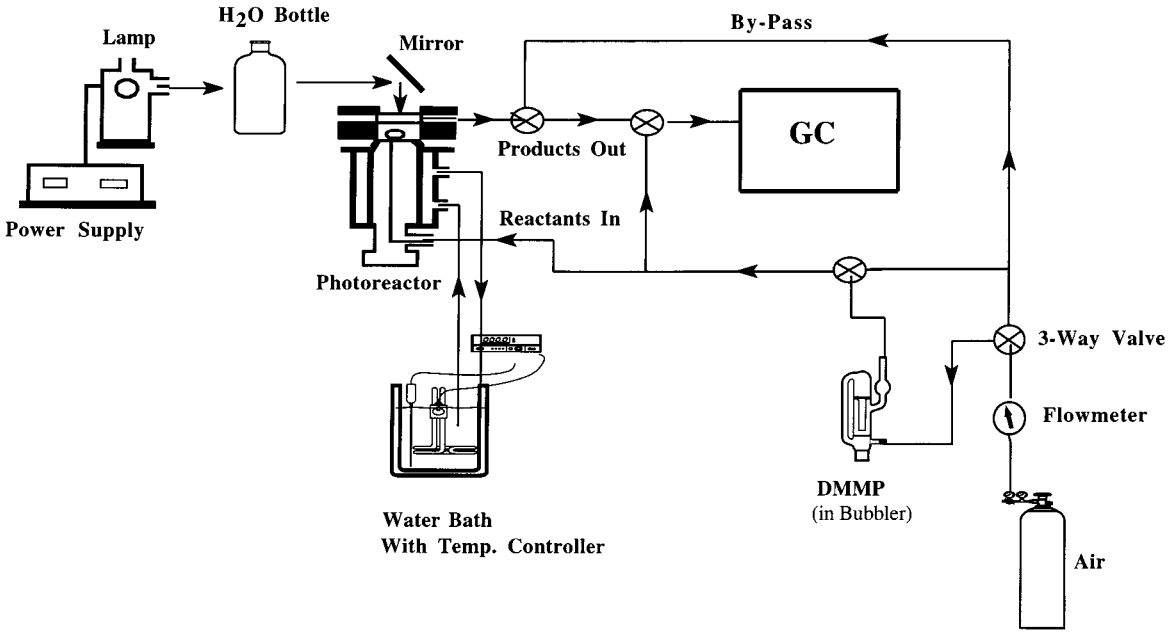

Figure 2. Experimental set-up used for photoreactions.

To confirm the presence of MPA and MMP in the IC analyses, standards were prepared and retention times were established. MPA was available commercially (Aldrich), whereas MMP needed to be synthesized in our laboratories. MMP was prepared according to literature procedures by partial hydrolysis of DMMP in aqueous NaOH solution.[7] In this procedure, 0.140 mol of DMMP was added to 150 mL of a 10% NaOH solution, and refluxed gently for 5 h. The solution was cooled slowly and acidified to pH = 2 with concentrated HCl. The solution was vacuum-distilled until a NaCl precipitate was observed in the distillation flask. The mixture was extracted several times with acetone and then filtered. The acetone extract was dried over $CaSO_4$ for several hours. The extract was refiltered and placed in a rotovap until ~15−20 mL of liquid remained. The sample was vacuum distilled, and a distillate was collected almost immediately. This distillation was necessary to remove trace amounts of acetone in the mixture. Following several more minutes of distillation, a small amount of liquid (~1 mL) was observed in the receiving flask. The liquid was identified as MMP and was confirmed by ^{1}H NMR studies.[21]

III. Results

A. AMO Preparation. The redox reaction between $KMnO_4$ and oxalic acid leads to the precipitation of AMO, which after drying has a composition of $K_{0.6}Mn_{0.93}O_2$.[20] The average Mn oxidation state in AMO has been determined to be 3.5−3.6, indicating that Mn exists in mixed valencies, most likely a mixture of 3^+ and 4^+, with some 2^+.[20] Powder X-ray diffraction patterns for AMO show no peaks, indicating that the material is amorphous. Pore size distribution measurements show that AMO is a porous material, having a surface area of 200 ± 10 m^2/g.[19]

Combustion analyses indicate that trace amounts of carbon (0.17%) exist in AMO. In the preparation of AMO, oxalic acid is oxidized to CO_2 and water, while the permanganate ion is reduced. Due to the vigorous nature of the reaction, some CO_2 becomes entrapped in the pores of the solid. The CO_2 may also be derived from unreacted oxalic acid remaining in the material.[18] This became apparent as CO_2 was initially detected when passing air over illuminated AMO. After a short period of time, the CO_2 would decrease. Therefore, prior to each experiment, air was passed over AMO under illumination to remove or desorb any CO_2 originating from the catalyst. After 30 min, no CO_2 was detected during photodesorption of AMO.

B. DMMP Reactions over AMO. DMMP reactions run in the absence of AMO indicate that no DMMP decomposition occurs when irradiated with light. DMMP reactions over AMO were typically run over time periods of about 5 h. Figure 3 a shows the fate of DMMP as a function of time. In the first 131 min, the reaction was performed under dark conditions. This was done because it was found that DMMP adsorbs on AMO in the dark. Therefore, it was necessary to allow the DMMP to adsorb in the dark until the surface was saturated and the inlet and outlet DMMP concentrations became equal. After this time, the lamp was turned on and the reaction was allowed to continue for another 141 min. The results show that under dark conditions, the concentration of DMMP initially decreases to ~17% of the original concentration, then climbs slowly back to the inlet concentration after 2 h. When the lamp is turned on, the DMMP concentration increases to over three times the original concentration and then quickly falls back to the original inlet concentration where it levels off. All runs were duplicated several times with fresh AMO to ensure reproducibility.

The chromatographic results using flame ionization detection also showed the presence of another peak, which was identified as methanol. Figure 3b shows the production of methanol (MeOH) as a function of time during DMMP reactions. Under dark conditions, small amounts of MeOH were produced, starting after 40 min of reaction. The average MeOH concentration during this portion of the reaction was ~1.2×10^{-3} mol %. When the lamp was switched on, the MeOH concentration increased dramatically to 3.33×10^{-2} mol %. The MeOH concentration then quickly decreased to 5.0×10^{-3} mol %, where it slowly leveled off.

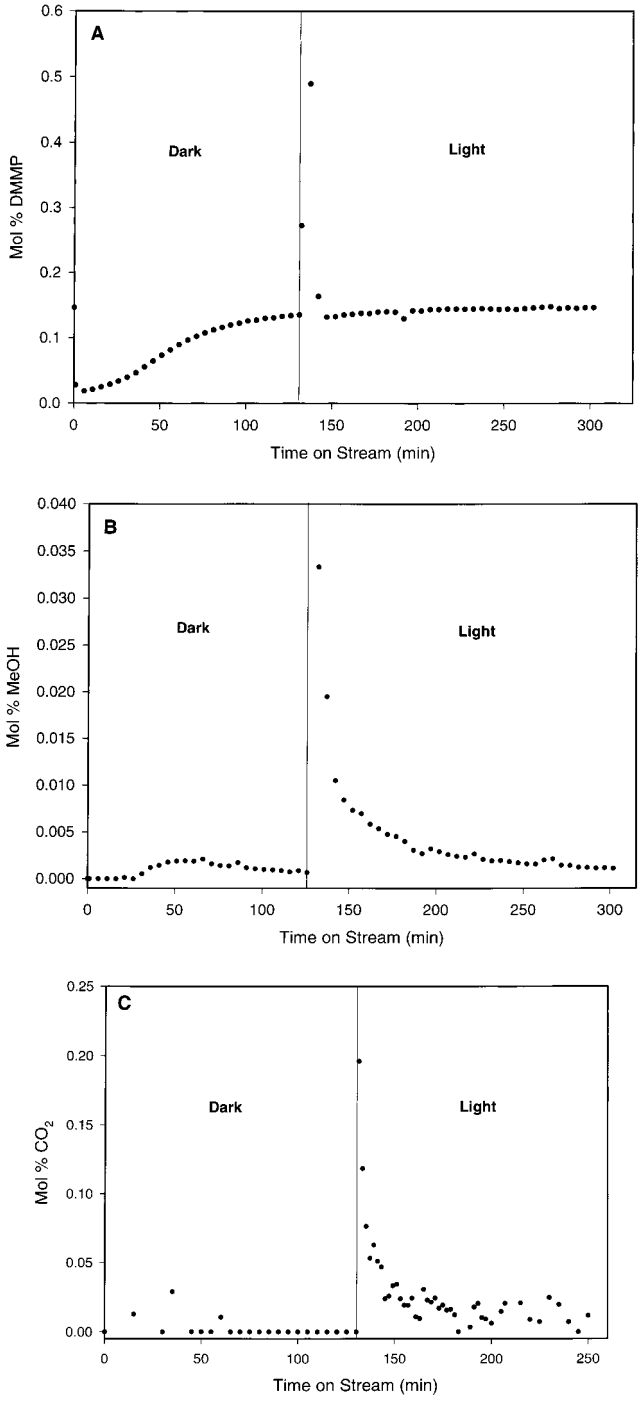

Figure 3. (a) Fate of DMMP vs time over AMO in photoreactions, (b) production of MEOH vs time over AMO in photoreactions, and (c) production of CO_2 vs time over AMO in photoreactions. Reaction conditions: 50 mg AMO, air flow rate = 30 mL/min, lamp power = 450 W.

Another product that formed during the DMMP reactions was CO_2. Figure 3c shows the formation of CO_2 during DMMP reactions. We do not see evidence of CO_2 formation under dark conditions. Some CO_2 peaks were observed toward the beginning of the reaction; presumably from noise or trace amounts of CO_2 remaining in the AMO. After the light was turned on there was a large increase in the CO_2 concentration, corresponding to 0.196 mol %. The concentration of CO_2 then quickly dropped to 0.017 mol %, where it remained fairly steady. At these low CO_2 concentrations, the analysis becomes somewhat difficult as the detection limit is approached.

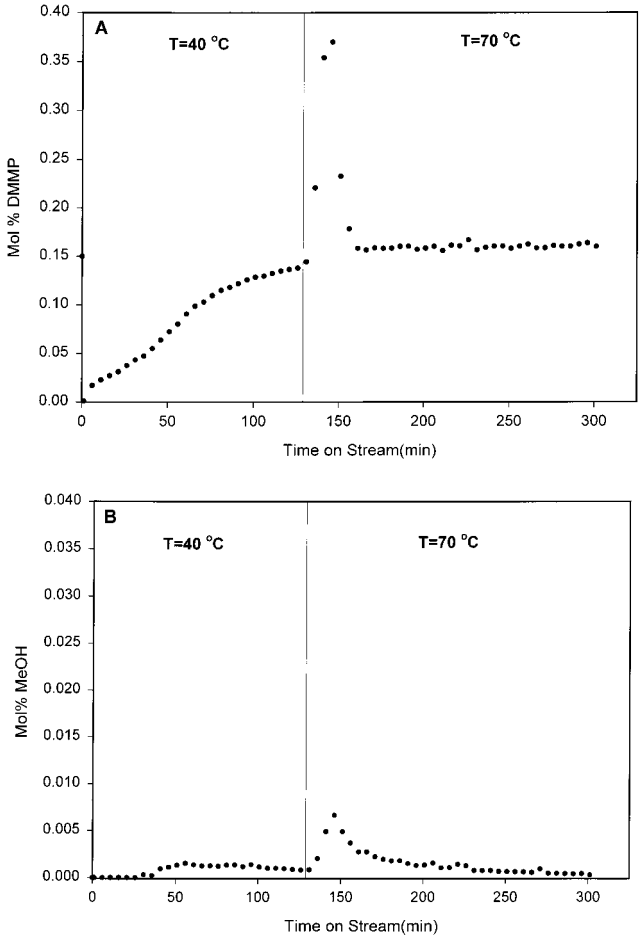

Figure 4. (a) Fate of DMMP vs time over AMO in thermal studies and (b) production of MeOH vs time over AMO in thermal studies. Reaction conditions: 50 mg AMO, air flow rate = 30 mL/min, 0−131 min = dark 40 °C, 132−272 min = dark, 70 °C.

C. Temperature Effects. Temperature measurements made inside the photoreactor indicate that light causes the temperature at the surface of AMO to increase to 70 °C. Since it is known that DMMP can decompose at high temperatures over metal oxides, experiments were performed under dark conditions at 70 °C to determine the thermal effects from light. In these experiments, the reaction was first run for 130 min in the dark at 40 °C. After this time, the temperature was increased to 70 °C (by flowing hot water through a heating/cooling jacket outside the reactor). The reaction was allowed to continue for several hours in the dark. The results for these experiments are shown in Figure 4, parts a and b. The fate of DMMP shows a similar trend to results from the photoreaction. However, as can be seen in Figure 4b, considerably less MeOH was produced in thermal reactions (max [MeOH] = 7.0×10^{-3} mol %). Under these conditions, no CO_2 was observed in thermal reactions. Turnover rates for DMMP reactions over AMO are listed in Table 1.

D. Regeneration of AMO. After several reactions with DMMP, AMO was collected (~90 mg) and placed in 100 mL of DDW and stirred for ~1 h. The sample was filtered and washed with DDW several times. The AMO sample was dried overnight in air at 110 °C, and

Table 1. Turnover Rates for DMMP Reactions over AMO

reaction	turnover rates*
dark, $T = 40$ °C (131 min)	1.19×10^{-3}
dark, $T = 70$ °C (141 min)	3.67×10^{-2}
dark, $T = 40$ °C (131 min)	1.20×10^{-3}
dark, $T = 70$ °C (141 min)	2.62×10^{-3}

*Turnover rate = (mol MeOH + mol CO_2)/mol Mn)(h). Reaction conditions are given in Figures 3 and 4.

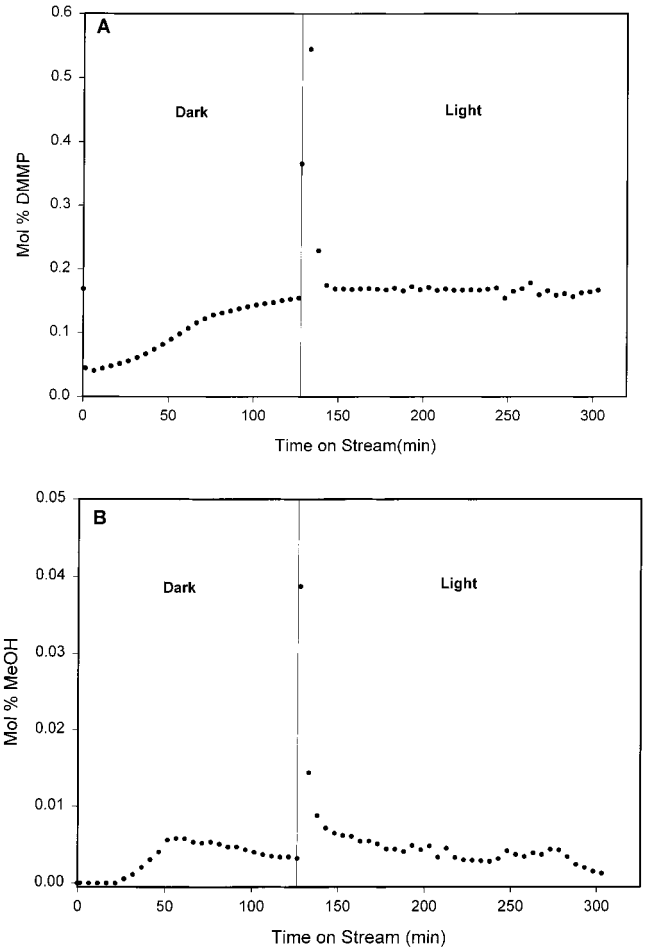

Figure 5. (a) Time course of DMMP in AMO regeneration studies and (b) production of MeOH vs time in AMO regeneration studies. Reaction conditions: 50 mg AMO, air flow rate = 30 mL/min, lamp power = 450 W.

the following day was retested as a catalyst in reactions of DMMP. Only DMMP and MeOH were analyzed in these experiments. Figure 5a shows the fate of DMMP during the reaction using regenerated AMO. This result is similar to that obtained when using fresh AMO. At the beginning of the reaction under dark conditions, the DMMP concentration decreases, although not as dramatically as in fresh AMO samples. The DMMP concentration then slowly increases to the inlet level. When the lamp was turned on, the DMMP concentration increases significantly as with fresh AMO and then levels off after several hours to concentrations near the inlet concentration.

Figure 5b shows the production of MeOH as a function of time in the regeneration experiments. The formation of MeOH also follows similar trends as fresh AMO. Under dark conditions, small amounts of MeOH (3.1×10^{-3} mol %) are formed, starting after 30 min. The MeOH concentration decreases slightly until the light is switched on. After the light is turned on, a large amount of MeOH (4.0×10^{-2} mol %) is initially observed. This corresponds to approximately the same amount of MeOH seen with fresh AMO samples. The production of MeOH then decreases as was observed with fresh AMO.

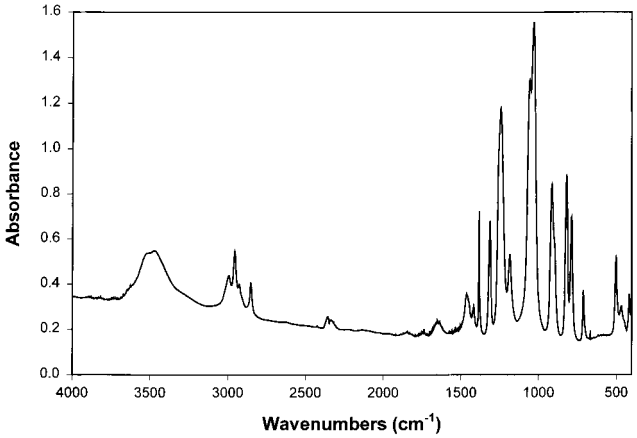

Figure 6. IR spectrum of liquid DMMP.

Table 2. IR Frequencies and Assignments for DMMP and Adsorbed DMMP on AMO after Reactions

	IR frequencies (cm^{-1})		
vibrational mode[a]	liquid DMMP	AMO dark reaction	AMO dark and light reaction
ν_a (CH_3P)	2997	2988 (0.002)	2988 (0.002)
ν_a (CH_3O)	2956	2956 (0.004)	2949 (0.002)
ν_s (CH_3P)	2930	2923 (0.003)	2926 (0.002)
ν_s (CH_3O)	2854	2852 (0.003)	2847 (0.002)
δ_s (CH_3P)	2997	2988 (0.002)	2988 (0.002)
ν (P═O)	1250	1225 (0.039)	1179 (0.035)
ρ (CH_3O)	1189	1184 (0.029)	1179 (0.035)
ν (CO)	1062	–	1052 (0.099)
ν (CO)	1036	1035 (0.147)	–
ρ (CH_3P)	914	917 (0.027)	898 (0.023)
ν (PO_2)	820	828 (0.022)	–
ν (PO_2)	789	793 (0.017)	797 (0.014)
ν (PC)	711	–	–

[a] Values for vibrational modes taken from Ref 11. ν = stretch, δ = deformation, ρ = rock. a = antisymmetric, s = symmetric. Numbers in parentheses denote absorbance units.

E. IR Analysis of Spent AMO. IR analyses of spent AMO were used to examine adsorbed DMMP species.

The IR spectrum of liquid DMMP was first measured for comparison and is shown in Figure 6. This was measured by placing a small amount of liquid DMMP onto a KBr pellet. The major peaks and their assignments are listed in Table 2. Peaks pertaining to DMMP occur between 3200 and 2600 cm^{-1} and between 1800 and 750 cm^{-1}. The higher frequency peaks are due to methyl group stretching vibrations, while the latter are due to C—O, C—P, and P═O stretching vibrations and methyl deformation vibrations.[11] Extra peaks occurring between 2300 and 2400 cm^{-1} are due to atmospheric CO_2, while the broad peaks around 3450 cm^{-1} are probably from small amounts of methanol or H_2O impurities in DMMP.

After reactions with DMMP, AMO was removed from the reactor and IR spectra were collected. To compare the effects of light on the adsorbed DMMP species, some AMO was removed after reaction with DMMP in the dark only (after 130 min). In Figure 7, IR spectra are shown for (a) AMO, (b) AMO after exposure to DMMP

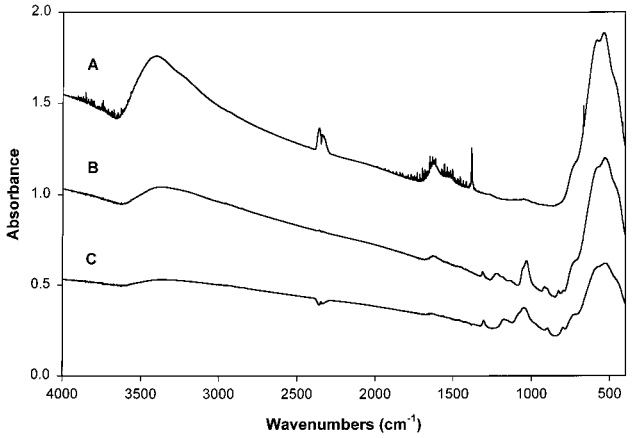

Figure 7. IR spectrum of (a) AMO, (b) AMO after reaction with DMMP in the dark, and (c) AMO after reaction with DMMP in the dark and light.

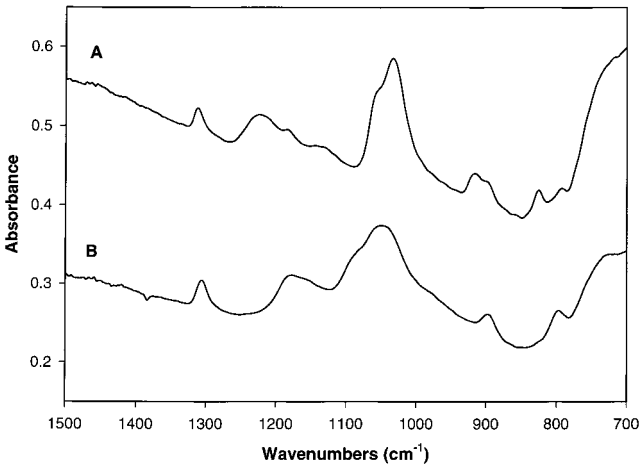

Figure 8. Lower frequency IR spectra of adsorbed DMMP species: (a) after reaction with DMMP in the dark, and (b) after reaction with AMO in the dark and light.

in the dark, and (c) AMO after exposure to DMMP in the dark and light. The assigned IR peaks for adsorbed DMMP species on AMO are given in Table 2. The IR spectrum of AMO shows an intense, broad peak centered around 500 cm^{-1}, which is due to Mn−O vibrations. Peaks between 1400 and 1800 cm^{-1}, and the broad peak at 3300 cm^{-1} are due to O−H vibrations, caused by adsorbed H_2O and hydroxyl groups on the AMO surface. Peaks are also observed between 2300 and 2500 cm^{-1}, which are due to atmospheric CO_2. The sharp peak at 1385 cm^{-1} is believed to be from an impurity in KBr.

The IR spectra of AMO after DMMP reactions in Figure 7 (parts b and c) both show the presence of many peaks associated with adsorbed DMMP. The most intense peaks occur at the lower frequencies (1800−750 cm^{-1}), while less intense peaks are observed at the higher frequencies (3200−2600 cm^{-1}). In addition, peaks caused by O−H vibrations are drastically reduced after reaction with DMMP. To see more detail, the lower frequency portion of the IR spectra are shown for AMO after reactions with DMMP in Figure 8. After dark reactions (part a), peaks can be seen at 1312, 1225, 1184, 1035, 917, 828, and 793 cm^{-1}. In the IR spectra of AMO taken after reactions done in the light (part b), similar peaks are observed; however, many of the peaks shift

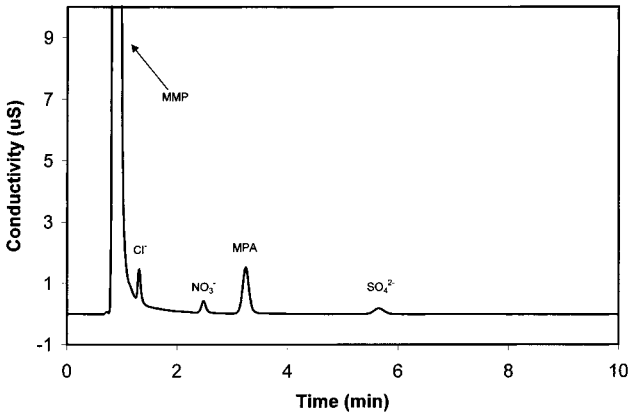

Figure 9. Ion chromatograph of an aqueous extract of AMO after reaction with DMMP in dark and light.

Table 3. Amount of MMP and MPA Produced During DMMP Decomposition Reactions

	reaction (mg/g)	
	MMP	MPA
dark (131 min)	26.54	0.10
dark (131 min) + light (141 min)	67.88	6.22
dark (272 min)	28.84	0.14

in frequency. In part b, peaks are observed at 1307, 1179, 1052, 898, and 797 cm^{-1}.

The higher frequency portion of the IR spectra of AMO after reactions with DMMP indicate that peaks appear much weaker in intensity than those of the lower frequency bands. Since these peaks are much weaker, the analysis becomes somewhat difficult. After dark reaction with DMMP, peaks are observed at 2988, 2956, 2923, and 2852 cm^{-1}. After reaction with light, similar peaks are observed; however, slight shifts to lower energies are noted, especially for CH_3O stretching frequencies.

F. Soxhlet and H_2O Extractions of Spent AMO. Soxhlet extractions in $CHCl_3$ of spent AMO after reactions in the dark and light showed the presence of DMMP, indicating that some DMMP is adsorbed molecularly. No attempt was made to quantify these data. A comparison was made between aqueous extracts of AMO after reactions with DMMP in the dark only, and with AMO after reaction in the dark and light. In Figure 9, an ion chromatogram is shown for an extract of AMO taken after reaction in dark and light. The IC analyses showed one major peak, identified as methyl methylphosphonate (MMP). A smaller peak was observed, which was identified as methylphosphonic acid (MPA). Additionally, small impurities from Cl^-, NO_3^-, and SO_4^{2-} were also observed. The IC results indicated that AMO extracts taken after dark and light reactions contained more MMP and MPA than extracts taken after dark reactions. Table 3 lists the amounts of MMP and MPA produced in DMMP decomposition reactions. To confirm that MMP and MPA are from DMMP and AMO, blank experiments were performed by treating DMMP with ultrasound and examining the products by IC. In these experiments, no MMP or MPA were observed, verifying that these products are from the decomposition of DMMP over AMO. No PO_4^{3-} was observed, indicative of incomplete decomposition of DMMP, MMP, and MPA.

IV. Discussion

A. Catalytic Results. The results from the DMMP reactions shown in Figure 3a indicate that there is a strong interaction between DMMP and AMO. Under dark conditions, DMMP is strongly adsorbed on the AMO surface. When irradiated with light, large amounts of DMMP are desorbed from the surface. This was apparent from the GC results as the DMMP concentration initially increased to three times the inlet concentration. Additionally, a condensate was observed to form on the inside of the quartz window of the reactor immediately following irradiation; presumably desorbed DMMP. These results suggest that a considerable amount of DMMP is molecularly adsorbed onto AMO and is desorbed immediately following irradiation. Since the vapor pressure of DMMP is extremely low (1.05 Torr), adsorption of DMMP on the AMO surface is favorable, especially at the low temperatures used in these reactions.

The results from Figure 3, parts b and c, show that DMMP reacts over AMO to form MeOH and CO_2. This indicates that in addition to molecular adsorption, some DMMP is adsorbed on AMO, followed by reaction to form products. The results from thermal decomposition reactions of DMMP over AMO (Figure 4, parts a and b) indicate that some thermal decomposition occurs. The turnover rate for the thermal reaction is an order of magnitude less than that for the photoreaction (see Table 1), suggesting that there is photoinduced decomposition of DMMP. The high activity initially observed after irradiation is immediately followed by fast deactivation. Under these conditions, no steady-state conversion was observed. The turnover rates for these reactions are quite low, suggesting that DMMP decomposition over AMO is stoichiometric and not catalytic.

We believe that these reactions are photoinitiated and that the initial activity is due to a photoevent. Additional thermal experiments carried out at temperatures which were measured during in situ irradiation (70 °C) showed significantly less (~8% photoproducts) product formation than during photolysis experiments. Such temperature measurements are consistent with previous studies using the same reactor in studies of decomposition of CH_3Br and oxidation of 2-proponol.[18−20] In both of these other photoreactions, there was clearly some but significantly less thermal conversion than photoconversion. A significant difference here, in the case of DMMP decomposition, is that deactivation and poisoning of the AMO catalyst is severe. We are currently devising ways to avoid such deactivation.

In catalytic oxidation studies of DMMP over metal oxides, strong deactivation is commonly observed.[1,6,12] A major concern in gas-phase catalytic studies of organophosphorus compounds over solids, is that poisoning of catalyst surfaces by PO_x species is favored, especially at lower temperatures. The total oxidation of DMMP can be represented by[6]

$$CH_3(CH_3O)_2PO + (x + 15)/2O_2 \rightarrow 3CO_2 + {}^3/_2\, H_2O + PO_x \quad (1)$$

In the total oxidation of DMMP, PO_x species cannot be removed from the catalyst unless temperatures >350 °C are used. This is because the most favored gaseous phosphorus oxide species (P_2O_5) has a sublimation point of around 350 °C.[6] In addition, the reaction of PO_x with H_2O can lead to the formation of phosphoric acid (i.e., H_3PO_4), which may also contribute to catalyst poisoning.

The results from the regeneration studies suggest that by washing spent AMO with H_2O, much of the phosphorus species can be removed. This is evident from Figure 4, parts a and b, as DMMP and MeOH plots of regenerated AMO showed similar trends as fresh AMO (Figure 3, parts a and b). Regeneration by washing TiO_2 after reaction with DMMP has also been shown to be successful.[22] In aqueous photocatalytic oxidations of DMMP over TiO_2, high conversion to H_3PO_4 was observed for several days.[13] These results indicate that H_2O may be very important in photocatalytic oxidations of DMMP over solids. This most likely occurs because H_3PO_4 and other organophosphates are soluble in H_2O, and water may help in desorbing adsorbed species from the catalysts, avoiding poisoning. Another advantage that H_2O has in photocatalytic oxidations is that reactive hydroxyl radicals are generated by photooxidation of H_2O. The hydroxyl radicals are often strong oxidants and are important in the total oxidation of many organic compounds.[13]

In our work, we have examined the effect of adding H_2O in the reaction. Experiments were performed by passing air through a bubbler containing H_2O and then mixing it with DMMP before the reactor. The results of these experiments showed that approximately the same amount of MeOH was produced compared with DMMP only reactions. These experiments suggest that a hydroxyl radical attack is not the predominant mechanism.

B. IR Analyses. The IR spectrum of AMO before DMMP reactions (Figure 7a) indicates that the AMO surface is hydroxylated. After reactions with DMMP (Figure 7, parts b and c), there is a large decrease in O−H and H_2O peaks, suggesting that DMMP either reacts with or displaces surface O−H groups on AMO. Previous IR studies have shown that photolysis of AMO can also remove H_2O from the surface.[18]

The results from the IR analyses of spent AMO (Figures 7b,c and 8 and Table 2) show the presence of many DMMP peaks. Many of these peaks are shifted toward lower energies. This is often indicative of bond weakening of adsorbed species on solids. The most pronounced shift is observed for the P═O vibration. In liquid DMMP, this peak appears at 1250 cm^{-1}. After reaction in the dark, the peak shifts to 1225 cm^{-1} and after reaction in the dark and light to 1179 cm^{-1}. This is strong evidence that the P═O moiety is involved in bonding to the AMO surface. Similar observations were recently observed in DMMP adsorption studies over Al_2O_3, MgO, and La_2O_3.[11] The interaction of P═O with Mn is consistent with a Lewis acid/base type adsorption mechanism. The phosphoryl oxygen is electron-rich,[7] and can act as a Lewis base, which can interact with Lewis acid sites on AMO (i.e. Mn^{3+}, Mn^{4+}). This leads to the formation of Mn−O═P bonds, which likely weaken the P═O bonds, consistent with the IR data. While this conclusion explains how the peak shifts from 1250 to 1225 cm^{-1}, it is not quite clear how light results in a further shift to 1179 cm^{-1}. Perhaps in light, the

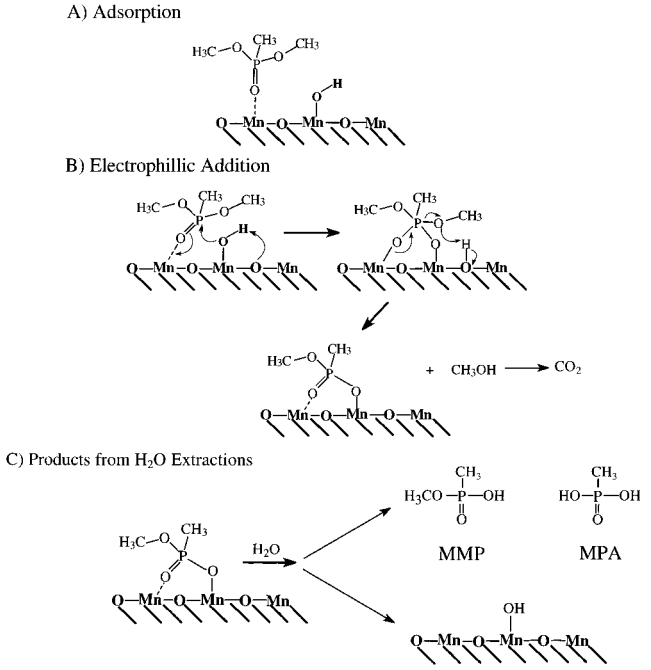

Figure 10. Scheme showing DMMP reaction mechanism on AMO surface.

phosphonate species orients differently, in a weaker interaction.

The IR spectra of Figure 8 indicate that the C−O stretching vibrations at 1062 and 1036 cm^{-1} become weaker and broader after reaction with DMMP in the light. This is consistent with the loss of methoxy groups (i.e., formation of MeOH). The peak at 1317 cm^{-1} corresponds to the CH_3P deformation. No intensity change was observed after DMMP reactions, suggesting that the P−CH_3 bond stays intact. However, this peak shifts slightly toward lower frequencies (10 cm^{-1}) after reaction in light, suggesting some weakening. The P−C stretch at 711 cm^{-1} cannot be analyzed in these studies due to interference from Mn−O peaks. Therefore, from the IR data, it is difficult to determine with certainty if P−CH_3 bonds are broken.

The peaks corresponding to PO_2 stretching vibrations at 820 and 789 cm^{-1} show several changes after DMMP reactions. After dark reactions with DMMP, the peak at 820 cm^{-1} shifts to 828 cm^{-1} and disappears after light reaction. The peak at 789 cm^{-1} shifts to higher energies after reaction with DMMP. These results suggest the formation of a new adsorbed species; perhaps a different PO_2 mode corresponding to the loss of methoxy groups (i.e., adsorbed methyl methylphosphonate).

C. Extraction Analyses and Mechanism. The Soxhlet extractions of AMO in $CHCl_3$ after reaction indicate that some DMMP is adsorbed molecularly or nondissociatively; however, H_2O extractions of spent AMO show that adsorbed DMMP reacts to form MMP and smaller amounts of MPA (Table 3). At the suggestion of a reviewer, an additional experiment was performed where the DMMP reaction was run over AMO in the dark for 272 min. These results show that roughly the same amount of MMP and MPA are produced as compared to dark only reactions after 131 min. The formation of MMP and MPA are consistent with the GC and IR data. A possible mechanism is shown in Figure 10. DMMP is first bonded to AMO via the phosphoryl oxygen. The second step involves electrophilic attack by the AMO surface on DMMP, leading to the loss of a methoxy group. This probably occurs by abstraction of hydrogen from AMO surface hydroxyl groups, which results in the evolution of MeOH and the formation of an adsorbed methyl methylphosphonate species. This species is then hydrolyzed in H_2O to form MMP and some MPA. This mechanism is similar to those observed in DMMP adsorption and decomposition studies by Mitchell et al. over Al_2O_3, MgO, and La_2O_3.[11]

Another possible mechanism involves superoxide anion radicals ($O_2^{\bullet-}$), which can form from the photoreduction of O_2. Superoxide anion radicals may react with DMMP as a nucleophile, causing hydrolysis and loss of a MeOH group. Further photoreactions were done in N_2, which showed that approximately the same amount of MeOH is produced in both cases. Since MeOH is produced in the absence of O_2, this suggests that a superoxide anion radical mechanism is not occurring. However, since AMO is known to release O_2 during photolysis, it cannot be completely ruled out that superoxide anion radicals do not form.

A reviewer has suggested that the formation of MeOH in the dark may be due to acid-catalyzed surface hydrolysis. This may be the case, since in the preparation of AMO, an acidic precursor is used (oxalic acid). It is therefore possible that the AMO surface is protonated. Several experiments were performed to examine this possibility. In one experiment, an unwashed sample of AMO was tested. It would be expected that an unwashed sample of AMO would be more acidic than washed samples of AMO. Another experiment was done using H^+−AMO, prepared by exchanging K^+ in AMO with NH_4^+. Following ion exchange, the sample was heated to evolve NH_3 leaving H^+−AMO.

In both cases, the enhancement of acidity of AMO to generate Brønsted sites led to materials that produced similar amounts of methanol. These data are somewhat inconclusive, since the number of acid sites was increased, but we have little information on the exact numbers, amounts, strengths, or types of sites introduced with this indirect method. In addition, the originally present acid sites are very likely still present and could still potentially give rise to methanol formation. We are unsure about the mechanism of methanol formation in the dark. At this point Brønsted acid, Lewis acid, or base sites cannot be ruled out.

The CO_2 formed in these reactions most likely comes from the photooxidation of methoxy groups of DMMP and possibly from the photooxidation of MeOH. Manganese oxide supported Al_2O_3 has been shown to be able to photooxidize MeOH to CO_2.[23] An experiment was done to determine if MeOH can be photooxidized to CO_2 over AMO. In this experiment, a small amount of liquid MeOH was placed on AMO, and then put into the photoreactor. When the sample was irradiated with light and air was passed over it, large amounts of CO_2 were observed. In thermal reactions done in the dark at 70 °C, no CO_2 was observed, suggesting that light is necessary for CO_2 formation. Since no phosphoric acid was detected in the AMO extracts, more conclusive

(23) Okzan, U. S.; Kueller, R. F.; Moctezuma, E. *Ind. Eng. Chem. Res.* **1990**, *29*, 1136−1142.

evidence is provided suggesting that no $P-CH_3$ oxidation is occurring.

V. Conclusions

To the best of our knowledge, this is the first report of DMMP decomposition reactions over manganese oxide materials. DMMP was found to strongly adsorb to AMO, with both physi- and chemisorption occurring. Initial irradiation of adsorbed DMMP on AMO shows that DMMP reacts to form CO_2 and MeOH. The CO_2 produced comes from the photooxidation of methoxy groups and not from oxidation of $P-CH_3$. The decomposition reaction occurs due to a combination of thermal and photoinduced effects. The strong adsorption of DMMP on the AMO surface leads to severe poisoning. Several products accumulate on the AMO surface, including MMP and MPA, which most likely contribute to the catalyst poisoning.

In the future we will try to improve the activity of gas- phase photoassisted DMMP decomposition reactions. One way in which this may be accomplished is by optimizing the catalyst synthesis. We are currently examining the addition of dopants, changing reactant concentrations, and the use of different reducing agents. To better understand AMO deactivation by DMMP and to improve conversion efficiencies, we are currently investigating thermal reactions (i.e., >70 °C) of DMMP over AMO.

Acknowledgment. We thank the U.S. Army and United Technologies Research Center, East Hartford, CT, for support of this work. This work was supported by the U.S. Army Research Office, under contract DAAH04-96-C-0067. The authors thank Dr. Jie Chen and Lisa Washmon for preliminary work done on this project. The authors also thank Dimitri Gumerov for collecting portions of the IC data.

CM980664W